TELLURIC EFFECTS ON PIPELINES

D.H. Boteler — Natural Resources Canada, 2617 Anderson Road, Ottawa, Canada

L. Trichtchenko — Natural Resources Canada, 2617 Anderson Road, Ottawa, Canada

H.-E. Edwall — Swedegas AB, Gamlestadsvägen 2-4, B15, 41502 Göthenborg, Sweden

Telluric Effects on Pipelines
Abstract

Telluric currents are produced in pipelines by the magnetic field variations that occur during geomagnetic disturbances. The telluric currents produce variations in pipe-to-soil potential (PSP) that can take the PSP outside the preferred range for cathodic protection. Use of higher resistance coatings on modern pipelines has increased the size of telluric PSP variations and increased the awareness of the telluric effects. Observations and modelling have shown that the size of the telluric PSP variations changes with position along a pipeline. This paper explains how to model telluric effects on pipelines and shows how pipeline characteristics such as pipeline length, coating conductance, and bends influence the telluric potentials. The modelling provides a framework for understanding telluric observations and can be used for telluric hazard assessments and for design of pipeline cathodic protection systems.

Tellurische Auswirkungen auf Rohrleitungen
Zusammenfassung

Tellurische Ströme entstehen in Rohrleitungen durch Schwankungen des Magnetfeldes, die bei geomagnetischen Störungen entstehen. Die tellurischen Ströme produzieren Schwankungen des Rohr/Boden-Potentiales, was dazu führen kann, dass Rohr/Boden-Potentiales ausserhalb des vorgeschriebenen Intervalles für katodischen Korrosionschutz fällt. Umhüllungsmaterialen mit einem höheren Umhüllungswiderstand zum Erdboden haben dazu geführt, dass die tellurischen Rohr/Boden-Potentiales Schwankungen bei neueren Rohrleitungen grösser geworden sind, wodurch die Aufmerksamkeit auf dieses Problem grösser geworden ist. Observationen und ausgeführte Modellierungen haben gezeigt, dass die Grösse der tellurischen Rohr/Boden-Potentiales Schwankungen an verschiedenen Positionen an einer Rohrleitung unterschiedlich sind. Diese Arbeit erklärt als Modell die tellurischen Auswirkungen auf Rohrleitungen sowie die Bedeutung von der Länge der Rohrleitung, der Beschichtung, der Leitfähigkeit, Rohrbiegungen und wie diese die tellurischen Potentiale beeinflussen. Die Modellierung bietet einen Rahmen für das Verständnis für tellurische Observationen und kann für Risikobewertungen und design von Rohrletiungssystemen mit katodischen Korrosionsschutz.

Effets telluriques sur les pipelines
Résumé

Les courants telluriques sont produits dans les pipelines par les variations du champ magnétique qui se survient lors de perturbations géomagnétiques. Les courants telluriques produisent des variations potentielles conduite-sol (PSP) qui peuvent prendre la PSP en dehors de la plage préférée pour la protection cathodique. L'utilisation de revêtements de résistance plus élevés sur les pipelines modernes a augmenté la taille de variations tellurique PSP et la prise de conscience des effets telluriques. Les observations et les modèles ont montrés que la taille des variations PSP telluriques change avec la position le long d'un pipeline. Cet article explique comment modéliser les effets telluriques sur les pipelines et montre comment leur caractéristiques comme la longueur, la conductance du revêtement, et les virages influences les potentiels telluriques. Le modèle fournit un cadre pour comprendre les observations telluriques et peut être utilisé pour les évaluations des risques telluriques et pour la conception de systèmes de conduites de protection cathodique.

Introduction

Telluric effects are a growing concern for maintaining proper cathodic protection for pipelines [1] and have been seen on pipelines in Europe [2, 3] and around the world [4, 5]. Modern pipelines are experiencing larger telluric PSP variations than older pipelines. Telluric effects have previously been seen mainly at high latitude locations [6 - 9] but are now also being seen on pipelines at lower latitudes [2 - 5].

Telluric currents in pipelines are driven by the electric fields produced by geomagnetic disturbances [10, 11]. The geomagnetic disturbances themselves are the result of a sequence of processes originating on the Sun. Solar radiation drives electric currents on the dayside of the Earth that creates a diurnal variation of the magnetic field. Solar eruptions of plasma also travel to Earth where their interaction with the Earth's magnetic field creates disturbances on a global scale and with localised enhancements at high latitudes associated with the aurora [12].

Variations of the magnetic field induce electric currents in the Earth and in conductors at the Earth's surface. The induced currents in the Earth also create magnetic fields that contribute to the magnetic disturbance. As a result the electric fields produced at the Earth's surface are influenced by the conductivity of the rock layers within the Earth. Different depths have different values of conductivity and, because lower frequencies variations penetrate deeper into the Earth, affect different frequencies components of the disturbances [13]. Surface variations in conductivity such as at geologic boundaries and at the coast also produce local enhancements of the electric field.

The electric fields drive telluric currents in pipelines and cause changes in the pipeline potential. Modelling methods have been developed that allow the potential to be determined for specified electric fields [14-16]. These show that the largest potential variations occur where the pipeline structure disrupts the flow of telluric currents along the pipeline, for example at bends, insulating flanges, and the ends of the pipeline. The size of the potential variations is influenced by the electrical properties of the pipeline. Modern use of coatings with higher electrical resistance has resulted in larger potential variations than on older pipelines.

This paper presents the developments in pipeline modelling and demonstrates how a pipeline network can be modelled to determine the telluric potentials produced by specified electric fields. To illustrate pipeline responses, simplified expressions are derived for electrically-long and electrically-short pipelines. These are used to show how the telluric potential varies with distance along the pipeline and at features such as bends, as well as showing how the coating and grounding resistances influence the size of the telluric potential. This information can then be combined with calculated electric fields to show the telluric potential variations that will occur during actual geomagnetic disturbances.

Pipeline Modelling

Geomagnetic induction in a pipeline can be modelled by considering the pipeline as a transmission line with series impedance *Z* and parallel conductance *Y*. These give the propagation constant γ and the characteristic impedance Z_0 of the pipeline.

$$\gamma = \sqrt{ZY} \qquad Z_0 = \sqrt{\frac{Z}{Y}} \tag{1}$$

The induced electric is represented in the transmission line model by a voltage source, E, in each distributed element (Fig. 1.). The voltage and current along the line are given by

$$\frac{dV}{dx} + ZI = E \tag{2}$$

and

$$\frac{dI}{dx} + YV = 0 \tag{3}$$

from which differentiation and substitution lead to the equations

$$\frac{d^2V}{dx^2} - \gamma^2 V = \frac{dE}{dx} \tag{4}$$

and

$$\frac{d^2I}{dx^2} - \gamma^2 I = -YE \tag{5}$$

If the electric field is assumed to be uniform within a section of pipeline, $dE/dx = 0$ and equation (4) becomes

$$\frac{d^2V}{dx^2} - \gamma^2 V = 0 \tag{6}$$

Equations (5) and (6) have solutions of the form

$$V = Ae^{\gamma x} + Be^{-\gamma x} \tag{7}$$

and

$$I = \frac{E}{\gamma Z_0} - \frac{A}{Z_0}e^{\gamma x} + \frac{B}{Z_0}e^{-\gamma x} \tag{8}$$

where *A* and *B* can be found from conditions at the ends of the line. At the start, *i*, of the section, *x=0*, equation (7) gives

$$V_i = A + B \tag{9}$$

while at the end, *k*, of the section, $x = L$, equation (7) gives

$$V_k = Ae^{\gamma L} + Be^{-\gamma L} \tag{10}$$

Combining these two equations gives

$$A = \frac{V_k - V_i e^{-\gamma L}}{e^{\gamma L} - e^{-\gamma L}} \tag{11}$$

and

$$B = \frac{V_i e^{\gamma L} - V_k}{e^{\gamma L} - e^{-\gamma L}} \tag{12}$$

Substituting for A and B in equation (7) for voltage gives

$$V = \left(\frac{V_k e^{\gamma L} - V_i}{e^{\gamma L} - e^{-\gamma L}}\right) e^{-\gamma(L-x)} + \left(\frac{V_i e^{\gamma L} - V_k}{e^{\gamma L} - e^{-\gamma L}}\right) e^{-\gamma x} \tag{13}$$

Similarly substituting for *A* and *B* in equation (8) for current gives

$$I = -\frac{1}{Z_0}\left(\frac{V_k e^{\gamma L} - V_i}{e^{\gamma L} - e^{-\gamma L}}\right) e^{-\gamma(L-x)} + \frac{1}{Z_0}\left(\frac{V_i e^{\gamma L} - V_k}{e^{\gamma L} - e^{-\gamma L}}\right) e^{-\gamma x} + \frac{E}{\gamma Z_0} \tag{14}$$

This represents the variation of voltage and current within a pipeline section.

To combine multiple sections into a model for a complete pipeline network it is convenient to represent each pipeline section by its equivalent-pi circuit as shown in Figure 1 where the circuit components are given by [16] as

$$Z' = Z_0 \sinh \gamma L \tag{15}$$

$$\frac{Y'}{2} = \left(\cosh \gamma L - 1\right) \frac{1}{Z_0 \sinh \gamma L} \tag{16}$$

$$E' = \frac{E}{\gamma} \sinh \gamma L \tag{17}$$

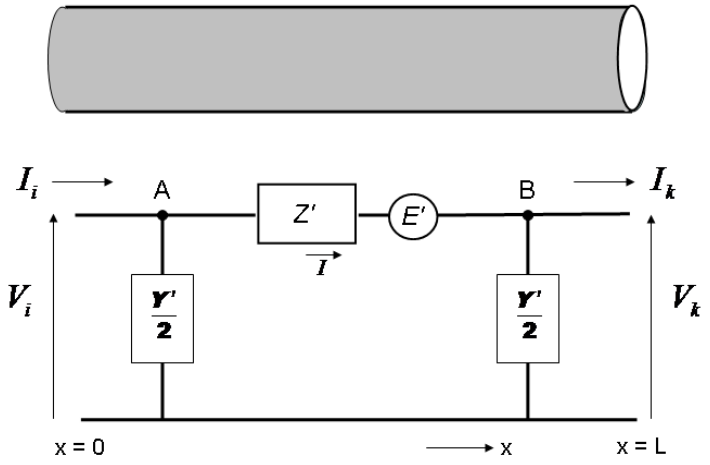

Figure 1. Equivalent-pi circuit for a pipeline section

To illustrate the pipeline network modelling, consider a pipeline comprising 3 sections, A, B and C with equivalent-pi circuits as shown in Figure 2a. At junctions between sections the admittance to ground *y'/2* from adjacent sections are in parallel and combine to give the total admittance to ground at that point. For example, in Fig. 2, the junction between sections A and B becomes node 12 and the junction between sections B and C becomes node 23, in the impedance network shown in Figure 2b.

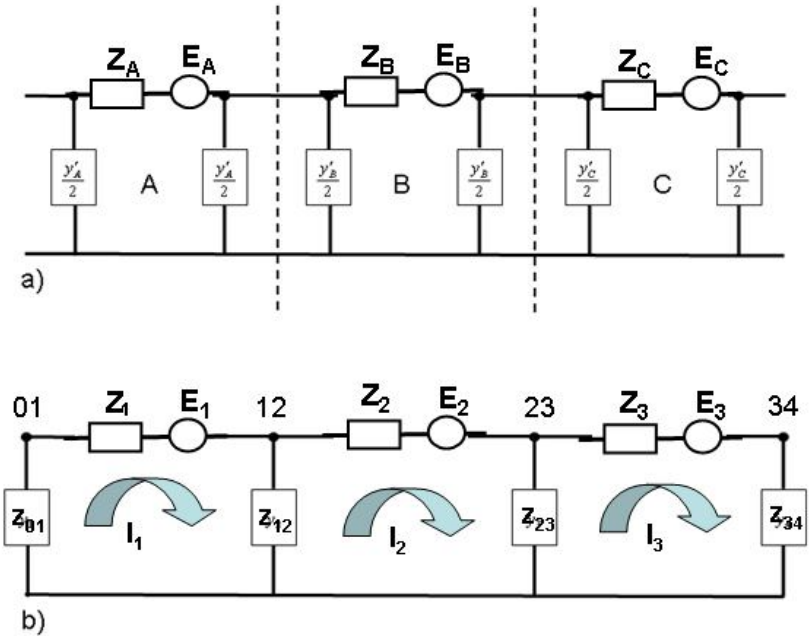

Figure 2. Pipeline represented as
a) Equivalent-pi sections for a pipeline.
b) a mesh impedance network

The impedance to ground at these nodes is then given by combining the admittances from the adjacent sections

$$\frac{1}{z_{12}} = y_{12} = \frac{y'_A}{2} + \frac{y'_B}{2} \qquad \frac{1}{z_{23}} = y_{23} = \frac{y'_B}{2} + \frac{y'_C}{2} \tag{18}$$

At the ends of the pipeline there is only the impedance to ground of one section, so:

$$\frac{1}{z_{01}} = y_{01} = \frac{y'_A}{2} \qquad \text{and} \qquad \frac{1}{z_{34}} = y_{34} = \frac{y'_C}{2} \tag{19}$$

The series impedance of the equivalent-pi sections becomes the series impedance of the corresponding section in the nodal network

$$z_1 = z_A \qquad z_2 = z_B \qquad z_3 = z_C \tag{20}$$

This then gives the mesh impedance network shown in Figure 2b which can be analysed to determine the currents in each loop and from those the voltage of each node. Applying Kirchhoff's voltage law that the algebraic sum of the voltages around any loop is zero, gives equations for each loop

$$\begin{aligned} z_{01}i_1 + z_1 i_1 + z_{12}(i_1 - i_2) &= e_1 \\ z_{12}(i_2 - i_1) + z_2 i_2 + z_{23}(i_2 - i_3) &= e_2 \\ z_{23}(i_3 - i_2) + z_3 i_3 + z_{34} i_3 &= e_3 \end{aligned} \tag{21}$$

Rearranging gives

$$\begin{aligned}(z_{01}+z_1+z_{12})i_1 - z_{12}i_2 &= e_1\\ -z_{12}i_1 + (z_{12}+z_2+z_{23})i_2 - z_{23}i_3 &= e_2\\ -z_{23}i_2 + (z_{23}+z_3+z_{34})i_3 &= e_3\end{aligned} \tag{22}$$

This can be written in matrix form:

$$\begin{bmatrix} z_{01}+z_1+z_{12} & -z_{12} & 0 \\ -z_{12} & z_{12}+z_2+z_{23} & -z_{23} \\ 0 & -z_{23} & z_{23}+z_3+z_{34} \end{bmatrix} \begin{bmatrix} i_1 \\ i_2 \\ i_3 \end{bmatrix} = \begin{bmatrix} e_1 \\ e_2 \\ e_3 \end{bmatrix} \tag{23}$$

Matrix inversion can then be used to give the loop currents from which the node voltages can be determined.

The modelling can be generalised to any pipeline network. Consider the impedance network shown in Figure 3 that represents the connection between two nodes A and B and connections to other nodes in the network.

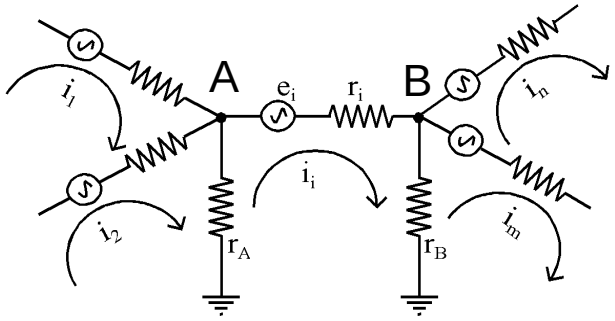

Figure 3. Mesh impedance network for modelling pipelines.

To develop the matrix equations we start by applying Kirchhoff's voltage law. Thus for loop *i*

$$(r_{Ai}+r_i+r_{Bi})i_i - \sum_{k=1(\neq i)}^{N} i_k r_{ki} = e_i \tag{24}$$

where the first term is the voltage drops produced by loop current i_i and the second term is the sum of contributions to voltage drops produced by currents in other loops that share a resistance to ground with loop *i*. In the example shown in Fig. 3, r_{1i} and r_{2i} have the value r_A, r_{mi} and r_{ni} have the value r_B. Currents in other loops do not contribute to the voltage drops in loop *i* so the "shared resistances" for these cases are set to zero. Equation (24) can be generalised to a matrix equation for all loops

$$[Z][I] = [E] \tag{25}$$

where

$$Z_{ii} = r_{Ai} + r_i + r_{Bi} \tag{26}$$

$$Z_{ki} = \pm r_{ki} \qquad \mathrm{k} \neq \mathrm{i} \tag{27}$$

with the sign in (27) depending on whether a loop current i_k is in the same or opposite direction to current i_i at the shared resistance. The currents are then found by taking the inverse of the impedance matrix and multiplying by the input driving induced emfs.

$$[I] = [Z]^{-1}[E] \tag{28}$$

The currents in the lines are given directly by the mesh currents. The currents to ground are the sum of all mesh currents sharing the resistance to ground. The node voltage is then obtained using this current to ground in Ohm's law, eg

$$v_A = r_A \sum_{k=1}^{N} i_k \qquad \text{for loops } k \text{ that include } r_A \tag{29}$$

These node voltages can then be used as the end voltages in equations (13) and (14) for each section to give the pipeline potentials and telluric current within each section of the pipeline.

Single Pipeline

To illustrate how pipeline characteristics affect the PSP produced by telluric currents consider a single straight pipeline of length L with grounding resistances R_{GA} and R_{GB} at the ends. Figure 4 shows the equivalent-pi circuit for the pipeline with the extra grounding resistances at the ends, shown by their equivalent admittance $Y_{GA} = 1/R_{GA}$ and $Y_{GB} = 1/R_{GB}$.

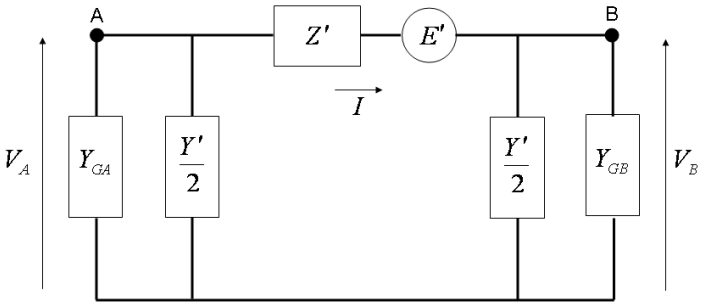

a)

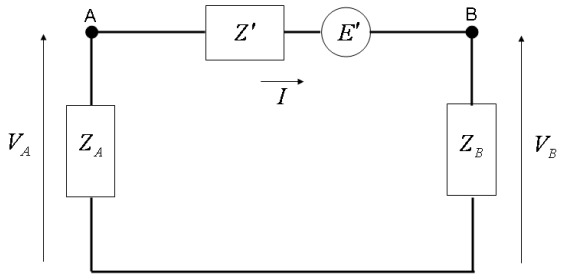

b)

Figure 4 a) Equivalent-pi circuit for a pipeline with grounds at the ends,
b) Reduced circuit

The admittance of the grounding at the end can be combined with the admittance of the equivalent-pi circuit to give the end impedances Z_A and Z_B given by

$$\frac{1}{Z_A} = Y_{GA} + \frac{Y'}{2} \qquad \frac{1}{Z_B} = Y_{GB} + \frac{Y'}{2} \tag{30}$$

The current around this loop is given by

$$I = \frac{E'}{Z_A + Z' + Z_B} \tag{31}$$

Therefore the end voltages are given by the voltage drops across the end impedances

$$V_A = -IZ_A = -\left(\frac{Z_A}{Z_A + Z' + Z_B}\right)E' \qquad V_B = IZ_B = \left(\frac{Z_B}{Z_A + Z' + Z_B}\right)E' \tag{32}$$

To illustrate the range of end voltage values that can occur it is useful to consider how these expresions simplify for electrically-long and electrically-short pipelines.

Electrically-Long Pipeline

For an electrically long pipeline, ie where $L > 4(1/\gamma)$, then $e^{\gamma L} >> 1 >> e^{-\gamma L}$ and the equivalent-pi circuit components given by equations (15) – (17) reduce to

$$E' = \frac{E}{\gamma}\left(\frac{e^{\gamma L}}{2}\right) \qquad Z' = Z_0\left(\frac{e^{\gamma L}}{2}\right) \qquad \frac{Y'}{2} = \frac{1}{Z_0} \tag{33}$$

In this case the end impedances in Figure 4 become

$$Z_A = \frac{Z_0 R_{GA}}{Z_0 + R_{GA}} \qquad Z_B = \frac{Z_0 R_{GB}}{Z_0 + R_{GB}} \tag{34}$$

The combined impedances then become

$$Z_A + Z' + Z_B = Z_0\left(\frac{R_{GA}}{Z_0 + R_{GA}} + \frac{e^{\gamma L}}{2} + \frac{R_{GB}}{Z_0 + R_{GB}}\right) \tag{35}$$

Regardless of the values for Z_0 , R_{GA} and R_{GB} the first and third terms will be less than one so, because of the condition that $e^{\gamma L} >> 1$, can be ignored. Thus equation (35) reduces to

$$Z_A + Z' + Z_B = Z_0\left(\frac{e^{\gamma L}}{2}\right) \tag{36}$$

The expresions for the end voltages then reduce to

$$V_A = -\left(\frac{R_{GA}}{Z_0 + R_{GA}}\right)\frac{E}{\gamma} \tag{37}$$

and

$$V_B = \left(\frac{R_{GB}}{Z_0 + R_{GB}}\right)\frac{E}{\gamma} \tag{38}$$

If there is no ground bed at the ends, i.e. $R_{GA} = R_{GB} = \infty$, then the voltages are

$$V_A = -\frac{E}{\gamma} \qquad V_B = \frac{E}{\gamma} \tag{39}$$

The voltages along the pipeline are given by equation (13) which, in the case of a long pipeline where $e^{-\gamma L} << 1$, reduces to

$$V(x) = V_A e^{-\gamma x} + V_B e^{-\gamma(L-x)} \tag{40}$$

Substituting for V_A and V_B then gives

$$V(x) = -\frac{E}{\gamma} V_A e^{-\gamma x} + \frac{E}{\gamma} V_B e^{-\gamma(L-x)} \tag{41}$$

This shows the PSP is largest at the ends of the pipeline and decreases exponentially with distance away from the end of the pipeline (Figure 5). The PSP are of different polarity at opposite ends of the pipeline. In this case the end voltage is dependent on the size of the electric field and the adjustment distance $1/\gamma$ of the pipeline. Under the condition of an electrically-long pipeline the maximum voltage at the end is independent of the actual length of the pipeline.

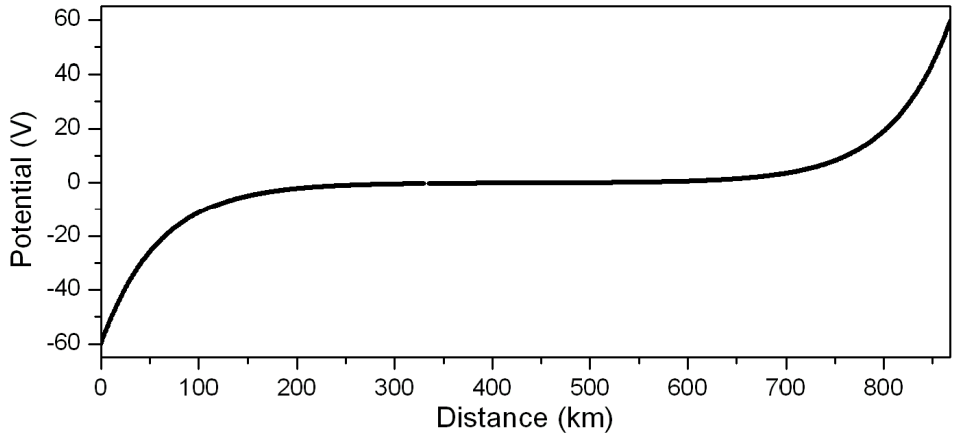

Figure 5. PSP variation with distance along an electrically-long pipeline.

Electrically-Short Pipeline

For pipelines that are short compared to the adjustment distance $1/\gamma$ then $|\gamma L| << 1$. In this case the expressions for the equivalent-pi components given by equations (15)-(17) reduce to

$$E' = EL \qquad Z' = ZL \qquad \frac{Y'}{2} = 0 \tag{42}$$

The end impedances in circuit (Figure 4b) then become

$$Z_A = R_{GA} \qquad Z_B = R_{GB} \tag{43}$$

The sum of the circuit impedances is then

$$Z_A + Z' + Z_B = R_{GA} + ZL + R_{GB} \tag{44}$$

The end voltages are then

$$V_A = -\left(\frac{R_{GA}}{R_{GA} + ZL + R_{GB}}\right)EL \qquad V_B = \left(\frac{R_{GB}}{R_{GA} + ZL + R_{GB}}\right)EL \tag{45}$$

If there are no ground connections then the grounding resistances at each end are infinite making the resistance along the pipeline insignificant. In this case the voltage expressions reduce to:

$$V_A = -\frac{EL}{2} \qquad V_B = \frac{EL}{2} \tag{46}$$

In the case of an electrically-short pipeline, the exponential terms can be approximated by $e^{\gamma x} = 1 + \gamma x$ and $e^{-\gamma x} = 1 - \gamma x$. Using these approximations equation (13) can be written

$$V = \left(\frac{V_k(1+\gamma L) - V_i}{2\gamma L}\right)(1 - \gamma(L - x)) + \left(\frac{V_i(1+\gamma L) - V_k}{2\gamma L}\right)(1 - \gamma x) \tag{47}$$

Multiplying out these terms and dropping terms involving $(\gamma L)^2$ or higher gives

$$V = V_k \frac{x}{L} + V_i\left(\frac{L - x}{L}\right) \tag{48}$$

Substituting for the end voltages from equation (46) this becomes

$$V = E\left(x - \frac{L}{2}\right) \tag{49}$$

This shows that for a short pipeline the voltage varies linearly along the pipeline as shown in Figure 6. The total voltage difference between the ends of the pipeline is equal to the product of the electric fieldand the length of the pipeline, EL. The maximum PSP in this case is $EL/2$. Thus the size of the end voltage is proportional to the length of the pipeline.

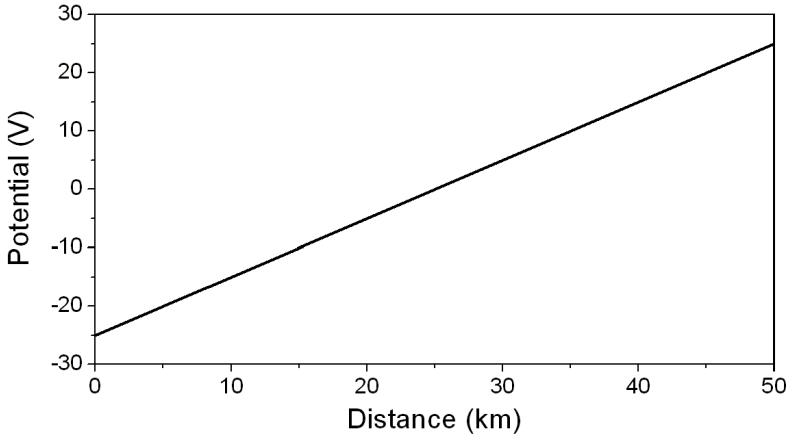

Figure 6. PSP variation with distance along an electrically-short pipeline.

Note, however, that this only applies while the electrically-short condition applies. As the pipeline length is increased the full expressions have to be used and ultimately the 'electrically-long' condition applies to give the dependence on pipeline length shown in Figure 7.

This has shown how the pipeline length affects the pipeline voltages. Other pipeline characteristics also affect the pipeline potentials produced by telluric currents. A key parameter that affects the size of the potentials is the coating conductance. Bends also affect where telluric potentials occur. These will be examined in the next sections.

Effect of Coating Conductance

The coating conductance influences both the characteristic impedance and propagation constant of a pipeline. The use of higher resistance coatings on modern pipelines decreases the coating conductance. This increases the characteristic impedance and decreases the propagation constant. For a long pipeline the end voltage is the multiple of the electric field and the adjustment distance 1/gamma (equation 39). The decrease in the propagation constant means an increase in the adjustment distance. Substituting this in equation (41) shows that this produces an increased voltage.

For short pipelines, equation (46) shows that the end voltage is independent of the coating conductance, while the "electrically-short" condition holds. However, for higher resistance coatings the adjustment distance will be greater, so the "electrically-short" condition holds for pipeline lengths greater than pipelines with lower resistance coatings. These factors give the variation of end potential with pipeline length for different coatings shown in Figure 7.

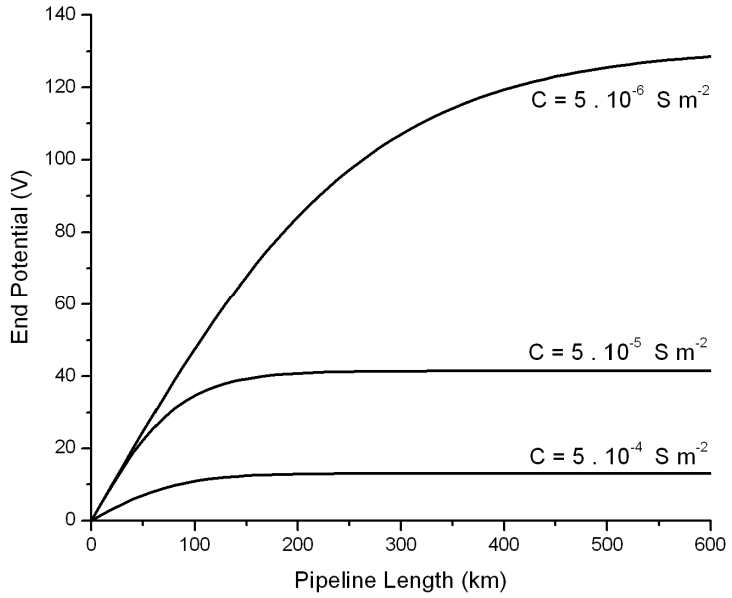

Figure 7. End potential as a function of pipeline length for pipelines with different coating conductance.

Discussion

The above modelling results shows that the largest telluric potential variations occur at the ends of pipeline sections. Thus the placement of insulating joints will influence where these telluric effects occur. This was first pointed out by Seager [17] who made telluric recordings on a long pipeline in northern Canada. He made initial recordings with a jumper connected around an insulating joint which made the pipeline electrically continuous from end to end. In this case the largest potentials occurred at the ends of the pipeline. A second set of recordings made with the jumper disconnected now found additional large potential variations on either side of the insulating joint.

More extensive tests of the effects of insulating joints were made by Edwall [18] on a pipeline in southern Sweden. This pipeline had been fitted with insulating joints because of the influence of stray currents from a high voltage direct current (HVDC) cable from Sweden to Germany.

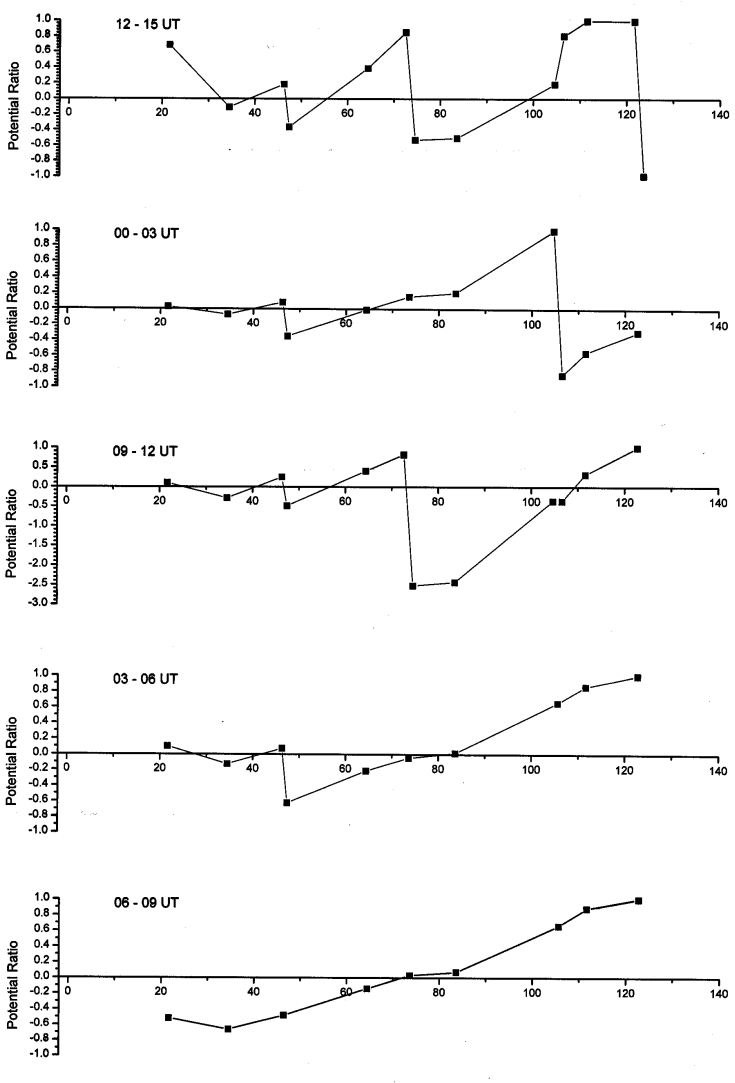

Figure 8. Relation between potential variations at different sites for different insulating joint configurations [18].

In a series of tests the insulating joints were fitted with jumper cables that were connected through clock-controlled switches. By switching in or out selected jumper cables the pipeline was switched into different configurations of sections with different lengths. Recordings of telluric potentials could then be separated into intervals with different pipeline configurations. The relation between the potential variations at different sites for the different pipeline configurations is shown in Figure 8.

For comparison with the telluric recordings a set of model calculations were made for the different pipeline configurations (Figure 9). These show that for all the pipeline lengths considered the pipeline was electrically short, thus there is a nearly linear variation in potential from end to end. It can also be seen that the longer pipeline sections have larger telluric potentials at the ends. The locations of these large potentials match the recorded potentials shown in Figure 8.

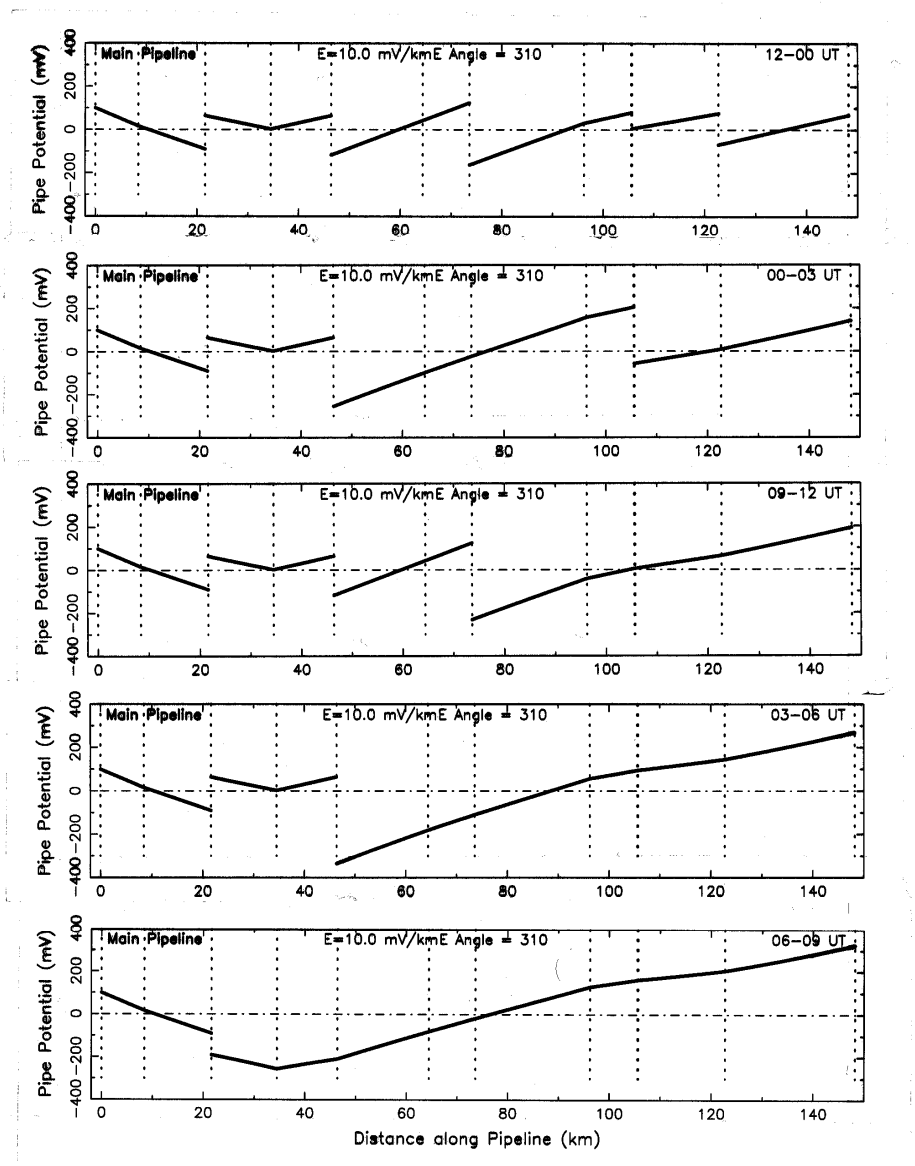

Figure 9. Model results for the Swedish pipeline for the different insulating joint configurations used during the observation period [18].

The modelling presented above shows the pipeline voltages produced with a variety of pipeline configurations by an electric field of a specified size and direction. During geomagnetic disturbances the telluric electric fields vary in both size and direction. Magnetic observatories make measurements of the northward, eastward and downward components of the magnetic field. These can be used with a model of the Earth conductivity structure to calculate the northward and eastward components of the electric field at the Earth's surface [14]. When the electric field reverses the opposite pipeline potential is produced. Thus as the electric field varies the pipeline potentials will also vary. For locations where the modelling shows potentials with opposite sign the time variations of the potential will be out of phase. This modelling provides a convenient way of calculating the pipeline potentials during past events and has been applied in online services [19, 20] and in telluric simulator software [21].

Conclusions

Telluric currents are produced in pipelines by natural geomagnetic field variations. As well as the size of the geomagnetic variation the frequency content of the variations and the conductivity structure of the underlying Earth influences the size of the telluric electric fields.

The telluric currents produce variations in pipeline potential that can interfere with cathodic protection of the pipeline. Progress in modelling of the electric characteristics of pipelines provides tools for assessing the pipeline potential variations that are produced.

Pipeline modelling shows that the pipeline response to telluric electric fields is strongly influenced by the length of the pipeline with respect to the pipeline adjustment distance. For “electrically short” pipelines the end potential is proportional to the telluric electric field and the pipeline length. For “electrically long” pipelines the end potential is independent of pipeline length and is given by the telluric electric field and pipeline adjustment distance.

The coating conductance has a strong influence on the adjustment distance of a pipeline. The use of higher resistance coatings on modern pipelines has led to larger telluric potential variations compared to older pipelines.

Telluric effects on pipelines are now being taken into account in the design and monitoring of cathodic protection systems for pipelines in many parts of the world. This is being made easier by the provision of online pipeline services and stand-alone simulation software.

Acknowledgements

This work was performed as part of Natural Resources Canada’s Public Safety Geoscience program with support from the Canadian Space Agency. Additional support was provided by the Panel on Energy Research and Development (PERD).

References

1. R.A. Gummow, "GIC effects on pipeline corrosion and corrosion control systems", J. Atmos. Solar Terr. Physics, 64, 1755–1764, 2002.

2. H. Brasse and A. Junge, "The influence of geomagnetic variations on pipelines and an application for large-scale magnetotelluric depth sounding", J. Geophys., 55, 31-36, 1984.
3. P. Hejda and J. Bochníček, "Geomagnetically induced pipe-to-soil voltages in the Czech oil pipelines during October-November 2003", Annales Geophysicae, 23, 3089-3093, 2005.
4. Martin, B.A., 1993. Telluric effects on a buried pipeline, Corrosion, 49, 343–350.
5. Osella, A., Favetto, A. & López, E., 1998. Currents induced by geomagnetic storms on buried pipelines as a cause of corrosion, J. appl. Geophys., 38, 219–233.
6. Campbell, W.H., "Observation of electric currents in the Alaska oil pipeline resulting from auroral electrojet current sources", Geophys. J. R. astr. Soc., 61, 437-449, 1980.
7. Henriksen, J.F., Elvik, R. and Granåsen, L., Telluric current corrosion on buried pipelines, Proc. 8thScandinavian Corrosion Congress, Helsinki, NKM8, vol 2, 167-176, 1978.
8. Trichtchenko, L., Boteler, D. H., Hesjevik, S. M., and Birketveit, O.: The Production of Telluric Current Effects in Norway, Paper 01314, Proceedings, CORROSION 2001, NACE International, Houston, 11–16 March 2001.
9. Pulkkinen, A., Viljanen, A., Pajunpää, K., and Pirjola, R., "Recordings and occurrence of geomagnetically induced currents in the Finnish natural gas pipeline network", J. Appl. Geophys., 48, 219–231, 2001a.
10. Lanzerotti L.J. and G.P.Gregori, Telluric currents: The natural environment and interaction with man-made systems, in The Earth's electrical environment, National Academy Press, Washington, DC, pp.232-257, 1986.
11. W.H. Campbell, "An interpretation of induced electric currents in long pipelines caused by natural geomagnetic sources of the upper atmosphere", Surveys in Geophysics, vol 8, 3, 239-259, September 1986.
12. D.H. Boteler, Telluric Currents and their Effect on Cathodic Protection of Pipelines, Paper No 04050, Proc. CORROSION/2004, NACE, Houston, March 2004.
13. Pirjola, R.: Review on the calculation of surface electric and magnetic fields and of geomagnetically induced currents in ground-based technological systems, Surveys in Geophysics, 23, 71–90, 2002.
14. Trichtchenko, L. and Boteler, D.H, Modelling of geomagnetic induction in pipelines Ann. Geophys., 20, 1063-1072, 2002, SRef-ID: 1432-0576/ag/2002-20-1063.
15. Pulkkinen, A., Pirjola, R., Boteler, D., Viljanen, A., and Yegorov, I, "Modelling of space weather effects on pipelines", J. Appl. Geophys., 48, 233–256, 2001b.
16. Boteler, D.H., A New Versatile Model of Geomagnetic Induction of Telluric Currents in Pipelines, Geophysical Journal International; doi: 10.1093/gji/ggs113, 2013.
17. Boteler, D.H. & Seager, W.H., 1998. Telluric currents: a meeting of theory and observation, Corrosion, 54, 751–755.
18. Edwall, H.-E. and Boteler, D.H., Studies of Telluric Currents on Pipelines in Sourthern Sweden, Paper 01315, Proceedings, CORROSION 2001, NACE, Houston, March 11-16, 2001
19. L. Trichtchenko, D.H. Boteler and P. Fernberg, "Space weather services for pipeline operations", Proceedings ASTRO 2008, CASI, Montreal, April 29-May 1 2008.
20. L. Trichtchenko, P. Fernberg and M. Harrison, "Use of geomagnetic data for evaluation of telluric effects on pipelines", Paper 14262, CORROSION 2010, Salt Lake City, NACE, Houston, 2010.
21. D.H. Boteler, L. Trichtchenko, C. Blais and R. Pirjola, "Development of a Telluric Simulator", Proceedings CORROSION 2013, March, NACE, Orlando, 2013.